AD-A042 361 BROWN UNIV PROVIDENCE R I DIV OF ENGINEERING F/G 20/11

ON DYNAMIC PLASTIC MODE FORM SOLUTIONS. (U)

JUN 77 P S SYMONDS, C T CHON N00014-75-C-0860

UNCLASSIFIED N00014-0860/2 NL

1 OF 1

AD A042361

END

DATE FILMED

8-77

DDC

NR-064-424
code 474

(12)

Division of Engineering
BROWN UNIVERSITY
PROVIDENCE, R. I.

# ON DYNAMIC PLASTIC MODE FORM SOLUTIONS

P. S. Symonds and C. T. Chon



National Science Foundation
Contract ENG74-21258

Office of Naval Research
Contract N00014-75-C-0860

N00014-0860/2

June 1977



(See 1473)

On Dynamic Plastic Mode Form Solutions

by P. S. Symonds[1] and C. T. Chon[2]

Abstract

The paper discusses the significance and calculation of dynamic plastic mode form solutions for small deflections of structures of rigid-perfectly plastic materials subjected to load systems of fixed distribution and magnitude. These solutions have separated form, with velocity the product of a scalar function of time by a vector-valued function of space variables. The relation is shown on the one hand to mode form solutions for a structure of viscoplastic material, and on the other hand to limit load solutions for those of perfectly plastic behavior. Numerical examples are given for circular plates of material obeying Tresca and Mises'laws.

1. Introduction. "Mode form" solutions of the equations governing the plastic response of a structure to dynamic loads are "particular integrals" in separated form: the velocity, for example, is the product of a function of space variables by a function of time. In this paper we are concerned with solutions of this type which hold throughout the motion, which we call "permanent" mode form solutions. They satisfy at all times the stated field equations of dynamics, kinematics, and material behavior, together with loading and boundary fixing conditions [1].[3] As will be seen, such solutions exist for certain idealizations of material behavior and loading, and when geometry changes are neglected in the governing equations. They are to be distinguished from "instantaneous" mode form solutions which satisfy the field equations only in a special sense [2 - 6]: regarding the displacement field as instantaneously fixed, and a scalar magnitude of the velocity field also as fixed, an instantaneous mode form solution has acceleration and velocity fields over the structure that are identical apart from a scalar factor. The common shape function satisfies the field

[1]Professor of Engineering, Brown University

[2]Research Associate, Brown University; now at Research Laboratory, General Motors Corporation

[3]See List of References

equations appropriate to the stated instantaneous displacement function and velocity magnitude.

Both types of mode form solutions have been used to obtain relatively simple approximate solutions of problems of structures loaded impulsively, i.e., by very short high-intensity pressure pulses whose effect can be specified by a field of initial velocities, with initial displacements taken as zero. Structures both of conventional plastic (time independent) and of rate dependent plastic (viscoplastic) material behavior have been treated. Permanent mode form solutions, when they exist, provide extremely simple solutions of initial motion problems that are appropriate for conditions in which geometry changes are negligible. However, in certain technically important cases the finite deflections have a large influence on the response and must be included. Approximate solutions for such cases have been constructed from a sequence of instantaneous mode form solutions, appropriate to successive stages in the response [5, 6]. In both types of application the specified initial velocity conditions are not satisfied exactly, but only in a "least squares" sense. This starting point also provides a measure of error, useful at least for comparing two such solutions.

Fundamental properties of dynamic-plastic structural motion underlie these methods [1-4]. The response of a structure to dynamic loading, however started, tends toward a mode form solution. Both types of mode solutions render a certain functional an extremum. Linear equations of dynamics and kinematics are presumed for these properties, which hold for a wide class of plastic/viscoplastic behavior.

Some of these properties are illustrated by a very simple structural model with two degrees of freedom [5, 7]. As shown in Fig. 1(a), the model simulates a simply supported beam by two mass particles connected by rigid massless rods, with joints at the two masses. The loads are forces $P_1$, $P_2$ applied to the masses. Deformation can occur only at the joints, and the material behavior is specified in terms of moment--rotation rate, etc. characteristics. For rigid-perfectly plastic behavior, the characteristic curve is shown in Fig. 1(c); fully plastic moments $\pm M_o$ are associated with rotation rates of corresponding sign and arbitrary magnitude. The rotation rates $\dot{\psi}_1$, $\dot{\psi}_2$ (Fig. 1(b)) are related to the transverse velocities $\dot{u}_1$, $\dot{u}_2$ by

$$\dot{\psi}_1 = \frac{1}{2\ell}(3\dot{u}_1 - \dot{u}_2) \quad ; \quad \dot{\psi}_2 = \frac{1}{2\ell}(-\dot{u}_1 + 3\dot{u}_2) \qquad (1a,b)$$

The equations of motion of the two masses can be written

$$P_1 - Y_1 = G\ddot{u}_1 \quad ; \quad P_2 - Y_2 = G\ddot{u}_2 \qquad (2a,b)$$

where $G$ is the mass of each particle and $Y_1$, $Y_2$ are the structural reaction forces; for small deflections, with notation as indicated in Fig. 1(d),

$$Y_1 = \frac{1}{2\ell}(3M_1 - M_2) \quad ; \quad Y_2 = \frac{1}{2\ell}(-M_1 + 3M_2) \qquad (3a,b)$$

We take the bending moments $M_1$, $M_2$ as satisfying

$$-M_o \le M_\alpha \le M_o \qquad (4)$$

where $\alpha = 1, 2$. Considering these inequalities, the locus of forces $Y_\alpha^L$ such that either $M_1$ or $M_2$ is equal to $\pm M_o$ is shown as curve ABCD of Fig. 2(a). By definition this is the "yield surface" of the structure. For $P_\alpha = P_\alpha^L = Y_\alpha^L$, unlimited slow deformation can occur, while load states $P_\alpha$ inside the curve can be supported without deformation; none occurs unless due to previous loading history. Kinematic relations obey the standard normality rule of yield surfaces; here the "strain rate" vectors of the structure are the velocity vectors $\dot{u}_\alpha = (\dot{u}_1, \dot{u}_2)$. For example, side AB of the structure yield curve corresponds to $M_1 = M_o$, $-M_o \leq M_2 \leq M_o$. For any load point not at either of the corner points A, B the velocity diagram has the shape shown in Fig. 2(b) with $\dot{u}_1 = 3\dot{u}_2$, since $\dot{\psi}_2 = 0$ for $|M_2| < M_o$. The velocity vector, as indicated in Fig. 2(a), is perpendicular to the line AB, whose equation is $3Y_1 + Y_2 = 4M_o/\ell$.

The discussion above assumes static behavior. Now we consider dynamic problems, the structure having non-zero accelerations $\ddot{u}_\alpha$ as well as velocities $\dot{u}_\alpha$. The dynamical equations (2) may be written in vector form with the dimensionless variables as

$$\underline{\hat{P}} - \underline{\hat{Y}} = \underline{\hat{\ddot{u}}} \tag{5}$$

$$\text{where} \quad \underline{\hat{P}} = \frac{\ell}{M_o}(P_1, P_2) \quad ; \quad \underline{\hat{Y}} = \frac{\ell}{M_o}(Y_1, Y_2) \quad ; \quad \underline{\hat{\ddot{u}}} = \frac{G\ell}{M_o}(\ddot{u}_1, \ddot{u}_2) \tag{6}$$

A typical dynamic case is shown in Fig. 2(a) for a load vector $\underline{\hat{P}}'$ which cannot be supported statically. The instantaneous stress vector $\underline{\hat{Y}}$ and velocity vector $\underline{\hat{\dot{u}}}$ must be related through the normality rule. Suppose the velocity vector has the direction of vector $\underline{\hat{\dot{u}}}'$. The stress state vector must correspond to the corner point B for this direction, which lies between the normals to the adjacent sides at point B. The acceleration vector $\underline{\hat{\ddot{u}}}$ is required by Eq. (5) to have direction and magnitude as shown. Evidently this is not a mode form motion, since the vectors $\underline{\hat{\ddot{u}}}$ and $\underline{\hat{\dot{u}}}$ are not parallel. However, it can be seen that if the load $\underline{\hat{P}}'$ remains constant the velocity vector must change with time until its direction and that of the acceleration vector become normal to side AB of the yield diagram. This "mode form" motion is indicated by the dashed vectors. This example illustrates the convergence property on which the mode approximation technique is based [1].

Several different types of mode form solution are illustrated in Fig. 2(b). They have the common feature that

$$\ddot{u}_\alpha = \Lambda(t)\dot{u}_\alpha \tag{7}$$

where $\Lambda$ is a scalar factor. We consider forces $P_1$, $P_2$ in fixed ratio to each other. Then the vector $\hat{\underline{P}}$ can be written as

$$\hat{\underline{P}} = \lambda\bar{\underline{P}} \tag{8}$$

where $\lambda$ is a scalar load factor and $\bar{\underline{P}}$ is a constant nominal load vector. In the example, $\bar{\underline{P}} = (1, -0.5)$. Figure 2(b) shows a number of cases corresponding to positive values of $\lambda$. At the plastic collapse or limit load with $\lambda = \lambda_L$, the acceleration is zero but the velocity is nonzero; this is case 3, with $\hat{\underline{Y}}^{(3)} = \hat{\underline{P}}^{(3)}$. The other extreme is that of $\hat{\underline{P}} = 0$, shown as case 1 with $\hat{\underline{Y}}^{(1)} = -\hat{\ddot{\underline{u}}}^{(1)}$. Here it is implied that some previous impulsive (or other) loading history has resulted in the mode pattern Fig. 2(b) with $\dot{u}_1 = 3\dot{u}_2$, so that the velocity vector has the direction of the normal to side AB and is parallel to $-\hat{\ddot{\underline{u}}}$. Note that the initial conditions and prior loading history are relevant only in the sense of causing a particular mode form to occur rather than another possible one. Evidently for $\lambda < \lambda_L$ the mode solution is not unique; for $\lambda = 0$ there are eight modes, with stress vector either perpendicular to one of the four sides or at one of the four corner points A, B, C, D. The case marked as case 2 has $\lambda^{(2)} < \lambda_L$. Here the mode is indicated by the velocity vector $\hat{\dot{\underline{u}}}^{(3)}$. In this case there are two possible mode solutions, the alternative mode shape having velocities proportional to ( -1, -3), with acceleration vector perpendicular to side BC of the yield curve, as indicated by dashed vectors in Fig. 2(b).

The case marked as case 4 has $\lambda^{(4)} > \lambda_L$ , so that the load state point lies outside the yield curve. For the example shown there is only one mode solution, the acceleration $\ddot{\hat{\underline{u}}}^{(4)}$ having the same direction as the velocity $\dot{\underline{u}}^{(4)}$. However, note that for $\lambda = \lambda_B$ the stress state point is at corner B. Case 5 has $\lambda^{(5)} > \lambda_B$ . The velocity vector can have any direction between the normals to the adjacent elements at B, so that the common direction of the acceleration and velocity vectors changes as $\lambda$ increases. For $\lambda \to \infty$ both approach the direction of the load vector $\hat{\underline{P}}$ .

2. Modes in a Circular Plate. To illustrate the requirements for mode form solutions of a continuous structure whose material exhibits either rigid-perfectly plastic behavior, or rigid-viscoplastic (strain rate dependent) behavior, we consider a circular plate of radius R , with a radially symmetric pressure p(r,t) applied transversely. As above, we consider only the plate in its initial configuration, i.e., we are not considering questions of finite deflections. The equation of motion is

$$\frac{\partial}{\partial r}\left[\frac{\partial}{\partial r}(rM_r) - M_\theta\right] = -pr + \bar{\rho}r\ddot{w} \tag{9}$$

Fixing conditions are, for example

$$w(R,t) = w'(R,t) = 0 \tag{10}$$

Initial conditions may also be stated as

$$w(r,0) = 0 \quad ; \quad \dot{w}(r,0) = \dot{w}^{o}(r) \tag{11}$$

In these equations, $r$ and $\theta$ are polar coordinates in the middle surface and $t$ is time; $w(r,t)$ is the transverse displacement, $w' = \partial w/\partial r$ the slope, $\dot{w} = \partial w/\partial t$ the velocity, and $\ddot{w}(r,t) = \partial^2 w/\partial t^2$ the acceleration; $M_r$ , $M_\theta$ are radial and circumferential bending moment per unit length, respectively; and $\bar{\rho}$ is the mass per unit area of middle surface.

The strain rate quantities relevant to the plate in bending are curvature rates $\dot{\kappa}_r$, $\dot{\kappa}_\theta$ defined so that the work-dissipation rate equation is

$$\int_0^R (p - \bar{\rho}\ddot{w})\, \dot{w}\, r dr = \int_0^R (M_r \dot{\kappa}_r + M_\theta \dot{\kappa}_\theta)\, r dr \tag{12}$$

Equations (9) and (12) are consistent with the following forms of the curvature rates in terms of the plate velocity

$$\dot{\kappa}_r = - \dot{w}'' \ ; \quad \dot{\kappa}_\theta = - \frac{1}{r} \dot{w}' \tag{13a,b}$$

We will write constitutive equations suitable either for rigid-perfectly plastic material or for one with strain rate sensitivity. Both behaviors can be treated by writing constitutive equations that are generalizations of the following form for simple tension:

$$\dot{\varepsilon} = \dot{\varepsilon}_o \left( \frac{|\sigma|}{\sigma_o'} \right)^{n'} \operatorname{sgn} \sigma \tag{14}$$

This homogeneous viscous form can represent adequately, over a range of strain rate, the more realistic inhomogeneous form

$$\dot{\varepsilon} = \dot{\varepsilon}_o \left[ \frac{|\sigma|}{\sigma_o} - 1 \right]^n \operatorname{sgn} \sigma \quad \text{for } |\sigma| \geq \sigma_o \tag{15a}$$

$$\dot{\varepsilon} = 0 \qquad\qquad \text{for } |\sigma| < \sigma_o \tag{15b}$$

This latter form is capable of close representation of curves for stress as function of strain rate at constant strain [8]; it is assumed that strain rate history effects are absent. The viscous form of Eq. (14) involves no yield condition. We need to write stress-strain rate relations which generalize Eq. (14) to appropriate forms for a thin plate in bending, in terms of bending moments $M_r$ $M_\theta$ and curvature rates $\dot{\kappa}_r$ , $\dot{\kappa}_\theta$ . We write for brevity

$m'_\alpha = M_\alpha/M'_o$ , $\dot{\xi}_\alpha = \dot{\kappa}_\alpha/\dot{\kappa}_o$ where $\alpha = r$ or $\theta$, $M'_o = \sigma'_o H^2/4$, $\dot{\kappa}_o = 4\dot{\varepsilon}_o/H$.
Then we can write

$$\dot{\xi}_\alpha = F^{n'} \frac{\partial F}{\partial m'_\alpha} = \frac{\partial \psi}{\partial m'_\alpha} \tag{16a}$$

where

$$F = \sqrt{m_r'^2 - m'_r m'_\theta + m_\theta'^2} \tag{16b}$$

$$\psi = \frac{1}{n'+1} F^{n'+1} \tag{16c}$$

and

$$m'_\alpha = G^{1/n'} \frac{\partial G}{\partial \dot{\xi}_\alpha} = \frac{\partial \omega}{\partial \dot{\xi}_\alpha} \tag{17a}$$

where

$$G = \frac{2}{\sqrt{3}} \sqrt{\dot{\xi}_r^2 + \dot{\xi}_r \dot{\xi}_\theta + \dot{\xi}_\theta^2} \tag{17b}$$

$$\omega = \frac{n'}{n'+1} G^{1+1/n'} \tag{17c}$$

These forms are derived by assuming a sandwich plate model of thickness $h = H/2$, $H$ being the thickness of the uniform plate. Each sheet of the sandwich plate is in plane stress, and has principal strain rate components $\dot{\varepsilon}_r$ , $\dot{\varepsilon}_\theta$ given in terms of stresses $\sigma_r$ , $\sigma_\theta$ by

$$\dot{\varepsilon}_\alpha = \dot{\varepsilon}_o \left(\frac{f}{\sigma'_o}\right)^{n'} \frac{\partial f}{\partial \sigma_\alpha} \; ; \quad \sigma_\alpha = \sigma'_o \left(\frac{g}{\dot{\varepsilon}_o}\right)^{1/n'} \frac{\partial g}{\partial \dot{\varepsilon}_\alpha} \tag{18a,b}$$

where $f = \sqrt{\sigma_r^2 - \sigma_r\sigma_\theta + \sigma_\theta^2}$ ; $g = \frac{2}{\sqrt{3}} \sqrt{\dot{\varepsilon}_r^2 + \dot{\varepsilon}_r\dot{\varepsilon}_\theta + \dot{\varepsilon}_\theta}$

and $\alpha = r, \theta$ . The forms of Eqs. (16, 17) are capable of close representation of strain rate behavior over appropriate strain rate ranges. If $n'$ is made very large while $\sigma'_o$ is taken as the static yield stress $\sigma_o$ , we obtain rigid perfectly plastic behavior.

We look for a mode form solution of Eq. (9) satisfying the edge conditions (10), kinematic relations (13), and constitutive equations (15), (17). We write the velocity as

$$\dot{w} = \dot{w}_*(t)\phi(r) \tag{19}$$

and take $\phi(0) = 1$, so that $\dot{w}_*(t)$ denotes the midpoint velocity. The curvature rates are then

$$\dot{\kappa}_r = \dot{w}_* k_r = \dot{w}_*(-\phi''); \quad \dot{\kappa}_\theta = \dot{w}_* k_\theta = \dot{w}_*(-\frac{1}{r}\phi') \tag{20}$$

The bending moments can also be written in separated variable form, because of the homogeneity of $\omega(\dot{\xi}_\alpha)$, as

$$M_r = \dot{\kappa}_o M_o' \dot{w}_*^{1/n'} \frac{\partial\tilde{\omega}}{\partial k_r} \; ; \quad M_\theta = \dot{\kappa}_o M_o' \dot{w}_*^{1/n'} \frac{\partial\tilde{\omega}}{\partial k_\theta} \tag{21a,b}$$

where $\tilde{\omega}(r) = \omega[k_\alpha(r)]$. The equation of motion then can be written as

$$\dot{\kappa}_o M_o' \frac{1}{r} \frac{\partial}{\partial r}\left[\frac{\partial}{\partial r}(r \frac{\partial\tilde{\omega}}{\partial k_r}) - \frac{\partial\tilde{\omega}}{\partial k_\theta}\right] = \dot{w}_*^{-1/n'}\left[\bar{\rho}\phi\ddot{w}_* - \lambda(t)\tilde{p}(r)\right] \tag{22}$$

Here we have further assumed that the load pressure has a constant distribution pattern over the plate, and have written

$$p(r,t) = \lambda(t)\tilde{p}(r) \tag{23}$$

For a rate sensitive material Eq.(22) can be "separated" only if the pressure distribution $\tilde{p}(r)$ is the same as the mode shape function $\phi(r)$ to within a constant factor. We conclude that apart from this highly special case, mode form solutions cannot exist when the plate is subjected to a pressure loading, even for the homogeneous viscous behavior. If $\tilde{p}(r) = 0$, separation of variables is possible since one can write

$$\frac{1}{\bar{\rho} r \phi} \frac{\partial}{\partial r}\left[\frac{\partial}{\partial r}\left(r \frac{\partial \tilde{\omega}}{\partial k_r}\right) - \frac{\partial \tilde{\omega}}{\partial k_\theta}\right] = \frac{1}{\dot{\kappa}_o M'_o} \frac{\ddot{w}_*}{\dot{w}_*^{1/n'}} = -A \tag{24}$$

where $A$ is a constant. It is seen that in this case the midpoint velocity decreases from its initial value $\dot{w}_*^o$ according to the expression

$$\dot{w}_*(t) = \left[(\dot{w}_*^o)^{1-\frac{1}{n'}} - \left(1 - \frac{1}{n'}\right) \dot{\kappa}_o M'_o At\right]^{\frac{n'}{n'-1}} \tag{25}$$

The shape function $\phi(r)$ must be obtained so as to satisfy the ordinary differential equation obtained by setting the left-hand side of Eq. (21) equal to $-A$. It may be solved by iterative methods [6, 8] without difficulty. When $\phi(r)$ has been obtained, the magnitude $A$ can be calculated from the energy-dissipation rate Eq.(12), which takes the form

$$-\dot{w}_*\ddot{w}_* \int_o^R \bar{\rho}\phi^2 r dr = \dot{\kappa}_o M'_o \left(\frac{\dot{w}_*}{\dot{\kappa}_o}\right)^{1+\frac{1}{n'}} \int_o^R [\tilde{\chi}(\phi)]^{1+\frac{1}{n'}} r dr \tag{26}$$

where $\tilde{\chi}(\phi) = \chi(k_\alpha) = \frac{2}{\sqrt{3}} \sqrt{(\phi'')^2 + \frac{1}{r}\phi'\phi'' + (\frac{1}{r}\phi')^2}$

because the dissipation rate can be expressed in terms of the homogeneous form $\omega$, using Euler's formula.

For rigid-perfectly plastic behavior we put $\sigma'_o = \sigma_o$, $n' \to \infty$. Then solutions in separated-variable form exist not only for the impulsive loading case with $\tilde{p}(r) = 0$, but for arbitrary $\tilde{p}(r)$, provided $\lambda(t) =$ constant. For this material the stress vector depends only on the direction of the strain rate vector, not on its magnitude, so that in a mode form solution the stresses are constant. Thus if the load factor $\lambda(t) = \tilde{\lambda} =$ constant, the acceleration is constant and given by

$$\ddot{w}_* = \frac{1}{\int_0^R \bar{\rho}\phi^2 rdr} \left[ \tilde{\lambda} \int_0^R \tilde{p}\phi rdr - \int_0^R (M_r k_r + M_\theta k_\theta) rdr \right] \tag{27}$$

The acceleration evidently can be negative (as in the impulsive loading case where $\tilde{\lambda} = 0$), or positive; zero acceleration is the case of "plastic collapse" in conventional plastic limit analysis theory. This range of possibilities has already been illustrated by the two-mass model.

3. Numerical Results for a Circular Plate. We consider henceforth a plate of rigid-perfectly plastic material subjected to a uniform pressure $p$ of various magnitudes. The plate has uniform mass density $\bar{\rho}$ per unit area, and constant thickness $H$. Integrating and assuming the mode form Eq. (19), the equation of motion Eq. (9) can be written in nondimensional form, with $m_r = M_r/M_o$, $m_\theta = M_\theta/M_o$, and putting $r/R \to r$, $0 \leq r \leq 1$, as

$$\frac{d}{dr}(rm_r) - m_\theta = -\left(\frac{pR^2}{M_o}\right)\frac{r^2}{2} + \left(\frac{\bar{\rho}\ddot{w}_* R^2}{M_o}\right)\int_0^r \phi rdr \tag{28}$$

The work-energy rate Eq. (24) becomes

$$\frac{pR^2}{M_o}\int_0^1 \phi rdr - \frac{\bar{\rho}\ddot{w}_* R^2}{M_o}\int_0^1 \phi^2 rdr = -\int_0^1 (m_r\phi'' + m_\theta \frac{\phi'}{r}) rdr \tag{29}$$

At a "hinge circle" the slope may be discontinuous, and the right hand side must then include a term

$$-r_1 m_r(r_1)\,\Delta\phi'(r_1) \equiv -r_1 m_r(r_1)[\phi'(r_1 + 0) - \phi'(r_1 - 0)] \tag{30}$$

for a hinge circle at $r = r_1$. We have boundary conditions at the edge $r = 1$:

$$\text{Simply supported edge} = \phi(1) = 0,\ m_r(1) = 0 \tag{31a}$$

$$\text{Clamped edge} = \phi(1) = 0,\ \phi'(1) = 0 \tag{31b}$$

At the center of the plate $r = 0$, $m_r(0) = m_\theta(0)$ by symmetry. We adopt the normalizing condition $\phi(0) = 1$, which merely defines $\dot{w}_*$ as the midpoint velocity of the plate.

(A) If we adopt Tresca's yield condition and the associated flow rule (Fig. 3), simple closed form solutions can easily be derived. The analysis is an obvious extension of that for the limit analysis problem, which corresponds here to putting $\ddot{w}_* = 0$. For the simply supported edge case, the stress states lie on segment AB of the yield curve, and all equations can be satisfied with velocity profile either conical in shape as in Fig. 4a, or with shape of a truncated cone as in Fig. 4b. The conical profile holds for

$$0 \le \frac{pR^2}{6M_o} \le 2 \tag{32}$$

and the relation between load and acceleration is

$$\frac{\bar{\rho}\ddot{w}_* R^2}{12M_o} = \frac{pR^2}{6M_o} - 1 \tag{33}$$

When $p$ is larger than the upper limit set by Eq. (32), a violation of the yield condition occurs at $r = 0$ ; thus the truncated cone field of Fig. 4b is required. This holds with

$$\frac{\bar{\rho}\ddot{w}_* R^2}{6M_o} = \frac{pR^2}{6M_o} = \frac{2}{(1-\eta^2)(1-\eta)} \ge 2 \tag{34}$$

Equation (33) furnishes the special cases of "free" decelerating motion, $\left(p = 0,\ \frac{\bar{\rho}\ddot{w}_* R^2}{M_o} = -12\right)$ and of the limit load pressure $p_L$ $\left(\ddot{w}_* = 0\ ,\ \frac{p_L R^2}{M_o} = 6\right)$, while Eq. (34) gives the parameter $\eta$ defining the (constant) shape of the response field for large pressures (more than twice the limit load magnitude).

For a clamped plate the stress states lie on segment AB of the yield curve for $0 \leq r \leq \xi$, but lie on BC for $\xi \leq r \leq 1$, in order to satisfy the edge conditions Eqs. (31b). The strain rate vector $(\dot{\kappa}_r, \dot{\kappa}_\theta) = \dot{w}_* (-\phi'', -\frac{1}{r}\phi')$ must be parallel to the $-m_r$ axis at $r = 1$, since $\phi'(1) = 0$, hence, the flow rule requires the stress state point at $r = 1$ to be point C of the Tresca diagram. Thus, if the pressure is not too large, the response field has a conical shape for $r \leq \xi$ and a logarithmic one for $\xi \leq r \leq 1$, as sketched in Fig. 4C. The mode function is given by

$$0 \leq r \leq \xi : \phi = 1 + \frac{r}{\xi(\ln \xi - 1)} \tag{35a}$$

$$\xi \leq r \leq 1 : \phi = \frac{\ln r}{\ln \xi - 1} \tag{35b}$$

The pressure and acceleration are expressed in terms of $\xi$ as follows:

$$\frac{pR^2}{6M_o} = \frac{14\xi^2 \ln \xi - 4\xi^2(\ln \xi)^2 - 8\xi^2 + 6}{\xi^2(2\xi^2 \ln \xi + 6 \ln \xi - 3\xi^2 + 3)} \tag{36a}$$

$$\frac{\bar{\rho}\ddot{w}_* R^2}{6M_o} = \frac{14\xi^2 \ln \xi - 4\xi^2(\ln \xi)^2 - 10\xi^2 - 6 \ln \xi + 6}{\xi^2(2\xi^2 \ln \xi + 6 \ln \xi - 3\xi^2 + 3)} \tag{36b}$$

provided $0.6201 \leq \xi \leq 0.8055$ (36c)

The important special cases are

Free deceleration, $p = 0 : \xi = 0.6201 ; \dfrac{\bar{\rho}\ddot{w}_* R^2}{M_o} = -23.58$ (37a)

Limit load pressure, $\ddot{w}_* = 0 : \xi = 0.7300 ; \dfrac{p_L R^2}{M_o} = 11.26$ (37b)

A violation of the yield condition at $r = 1$ will occur for $\frac{pR^2}{M_o} > 22.49$, corresponding to $\xi > 0.8055$, if the above mode field is retained. The mode shape for large pressure magnitudes has constant velocity in an interior region as sketched in Fig. 4d. The mode function is

$$0 \leq r \leq \eta : \qquad \phi = 1 \tag{38a}$$

$$\eta \leq r \leq \xi : \qquad \phi = \frac{r + \xi \ln \xi - \xi}{\xi \ln \xi - \xi + \eta} \tag{38b}$$

$$\xi \leq r \leq 1 : \qquad \phi = \frac{\xi \ln r}{\xi \ln \xi - \xi + \eta} \tag{38c}$$

The load pressure and acceleration are related to $\eta$ and $\xi$ by

$$\frac{pR^2}{M_o} = \frac{\bar{\rho}\ddot{w}_* R^2}{M_o} = \frac{12\xi\ (\xi \ln \xi - \xi + \eta)}{\eta^4 - 2\xi\eta^3 + 2\xi^3\eta - \xi^4} \tag{39a}$$

$$(1 - \ln \xi)\eta^4 - 2\xi\eta^3 + (5\xi^3 - 3\xi - 2\xi^3 \ln \xi)\eta - (\xi^4 + 3\xi^2 \ln \xi) = 0 \tag{39b}$$

$$\text{provided} \quad \eta \geq 0,\ \xi \geq 0.8055,\ \frac{pR^2}{M_o} \geq 22.49 \tag{39c}$$

These results for the static limit pressure and for the free deceleration of a circular plate, obeying the Tresca yield condition, are of course well known, being due to Hopkins and Prager [9, 10] and Wang and Hopkins [11]. They are here cited as special cases of the general family of mode form solutions of this structure.

(B) If we instead adopt Mises' yield condition and associated flow rule, the calculation of mode shapes and accelerations must be carried out by a numerical method. We have done this by several iterative schemes and by a finite element program. Iterative schemes are easy to devise in an intuitive way, and usually work well in some range. They have an unfortunate habit of failing to converge outside of certain ranges of the parameters involved. When they do converge, they furnish essentially exact solutions at small computer cost. Here we briefly outline the iterative scheme which was found to work well in the present problem over a wide range of the relevant parameters. Our finite element solution was much more expensive. It is mentioned here because in subsequent work extending the mode technique to large deflections it was found to have a somewhat wider domain of convergence than the iteration scheme.

The iterative solution of the present problem, where only small deflections are considered, was that used in the determination of mode shapes in a visco-plastic plate [6]. The use of a homogeneous viscous representation of visco-plastic behavior has been outlined above. Equations (16) and (17) respectively furnish strain rates and bending moments in terms of material parameters $\dot{\varepsilon}_o$, $\sigma_o'$, $n'$. The last two are written in terms of the constants of Eq. (15a) as

$$\sigma_o' = \mu\sigma_o \; ; \quad n' = \nu n \tag{40}$$

where $\sigma_o$, $n$ are obtained with $\dot{\varepsilon}_o$ from tests over a range of strain rates, and $\mu$, $\nu$ are factors which enable the homogeneous viscous forms to match test data in a particular range of strain rates. We have used the following for a conservative and accurate matching with strain rate test data [5, 6, 8]:

$$\nu = \frac{1 + \beta^{1/n}}{\beta^{1/n}} \; ; \quad \mu = \frac{1 + \beta^{1/n}}{\beta^{1/\nu n}} \tag{41a,b}$$

where $\beta = \dot{\varepsilon}_e/\dot{\varepsilon}_o$, $\dot{\varepsilon}_e$ being the effective strain rate at which the two representations are matched. The function $g(\dot{\varepsilon}_\alpha)$ in Eqs. (18) serves as $\dot{\varepsilon}_e$ in a plane stress problem, while $G(\dot{\kappa}_\alpha)$ serves as $\beta$ in a small deflection plate problem. As previously mentioned, rigid-perfectly plastic behavior is obtained by taking $\mu = 1$ and $\nu$ very large, corresponding to putting $\beta \to 0$ in Eqs. (41). We outline the iterative scheme in the form for a homogeneous viscous behavior, so that either a rate sensitive plate with $p = 0$ (impulsive motion) or a rigid-perfectly plastic plate with arbitrary $p$ can be treated.

The equation of motion (28) may be integrated again and put in the form

$$m_r = \int_o^r \frac{1}{r'}(m_\theta - m_r)dr' - \frac{1}{4}\bar{p}r^2 + \bar{\bar{w}} \int_o^r dr' \left(\frac{1}{r'}\int_o^{r'} \phi\hat{r}d\hat{r}\right) + C_1 \tag{42a}$$

where

$$\bar{p} = \frac{pR^2}{M_o} \quad ; \quad \bar{\bar{w}} = \frac{\bar{\rho}W_* R^2}{M_o} \tag{42b}$$

and $C_1$ is a constant of integration. Now, from the constitutive equations (17), with the mode solution form Eq. (19) and the curvature rate expressions Eqs. (20), the dimensionless moments are

$$m_r = -\frac{4}{3}\mu\left(\frac{\dot{W}_*}{\dot{\kappa}_o R^2}\right)^{1/n'} \chi^{1/n'-1}(\phi'' + \frac{1}{2r}\phi') \tag{43a}$$

$$m_\theta = -\frac{4}{3}\mu\left(\frac{\dot{W}_*}{\dot{\kappa}_o R^2}\right)^{1/n'} \chi^{1/n'-1}(\frac{1}{2}\phi'' + \frac{1}{r}\phi') \tag{43b}$$

where

$$\chi = \frac{2}{\sqrt{3}}\left[(\phi'')^2 + \frac{1}{r}\phi'\phi'' + (\frac{1}{r}\phi')^2\right]^{1/2} \tag{43c}$$

using Eq. (43a) in Eq. (42a), we write

$$\phi'' + \frac{1}{2r}\phi' = \frac{\int_o^r \frac{1}{r'}(m_\theta - m_r)dr' - \frac{1}{4}\bar{p}r^2 + \bar{\bar{w}}_* \int_o^r dr'\left(\frac{1}{r'}\int_o^{r'}\phi\hat{r}d\hat{r}\right) + C_1}{-\frac{4}{3}\mu\left(\frac{\dot{W}_*}{\dot{\kappa}_o R^2}\right)^{1/n'}\chi^{1/n'-1}} \tag{44a}$$

with

$$m_\theta - m_r = -\frac{4}{3}\mu\left(\frac{\dot{W}_*}{\dot{\kappa}_o R^2}\right)^{1/n'}\chi^{1/n'-1}\left[-\frac{1}{2}\phi'' + \frac{1}{2r}\phi'\right] \tag{44b}$$

We may consider a rigid-perfectly plate by putting $\mu = 1$ and taking $n' = \nu n$ very large so that the velocity $\dot{w}_*$ disappears from the right hand side. Alternatively, to consider a viscoplastic material we must put $\bar{p} = 0$ ; again $\dot{w}_*$ is eliminated since $\ddot{w}_*/\dot{w}_*^{1/n'}$ can be taken constant and obtained from Eq. (26). In either case,

$$\phi'' + \frac{1}{2r}\phi' = \frac{1}{\sqrt{r}}\frac{d}{dr}\left(\sqrt{r}\phi'\right) = \overset{<1>}{R}(r,C_1) \tag{45}$$

where the right-hand side is known numerically, apart from the constant $C_1$ , if a first approximation $\overset{<1>}{\phi}(r)$ is inserted in the right-hand sides of Eqs. (41) and in Eq. (26). Integrating Eq. (45),

$$\phi' = \frac{1}{\sqrt{r}}\int_0^r \sqrt{r'}\,\overset{<1>}{R}(r',C_1)dr' \tag{46}$$

(An integration constant has been taken as zero for a plate that is continuous at $r = 0$.) The constant $C_1$ must be determined from the edge condition at $r = 1$: for a simply supported plate the left-hand side of Eq. (44a) vanishes, while for a clamped plate that of Eq. (46) is zero. In either case we obtain

$$\phi'(r) = \overset{<1>}{S}(r) \tag{47}$$

where $\overset{<1>}{S}$ is the right-hand side of Eq. (46) with the constant $C_1$ evaluated

and

$$\phi(r) = -\int_r^1 \overset{<1>}{S}(r')dr' \tag{48}$$

Finally, a second approximation $\overset{<2>}{\phi}$ is obtained by multiplying the right-hand side of Eq. (48) by a factor which renders $\overset{<1>}{\phi}(0) = 1$ , giving

$$\overset{<2>}{\phi}(r) = \int_r^1 \overset{<1>}{S}(r')dr' \Bigg/ \int_0^1 \overset{<1>}{S}(r')dr' \tag{49}$$

This is put in place of $\phi^{<1>}(r)$ and the cycle is repeated. Convergence is shown by the approach of $\bar{\bar{w}}_*$ for chosen $\bar{p}$ (or of $\bar{\bar{w}}/\dot{w}_*^{1/n'}$ for $\bar{p} = 0$) to a constant value, and of the normalizing factor $-\int_0^1 S(r')dr'$ to unity.

The midpoint acceleration as function of load pressure is shown nondimensionally in Fig. 5 for both yield conditions and both types of edge constraint. The shapes of the mode form responses for the plates governed by Mises' yield condition are illustrated in Figs. 6 and 7. These evidently are close to the shapes for the Tresca material, for $pR^2/6M_o$ greater than about 20.

## Conclusions

Mode form solutions of structures undergoing dynamic plastic deformation have utility in approximation techniques; they have basic significance as "natural" response patterns to which structures with arbitrary starting conditions tend to converge. In this paper we have illustrated sufficient conditions of loading, material behavior, etc. for such solutions to exist. We have discussed examples of their calculation and have illustrated the links between response of dynamically loaded structures and static limit load-plastic collapse analysis. It is hoped that the discussion will promote understanding and use of these properties of dynamic plastic response.

REFERENCES


1 Martin, J. B., and Symonds, P. S., "Mode Approximations for Impulsively Loaded Rigid-Plastic Structures," Journal of Engineering Mechanics Division, Proceedings, ASCE, Vol. 92, 1966, pp. 43-66.

2 Lee, L. S. S., and Martin, J. B., "Approximate Solutions of Impulsively Loaded Structures of a Rate-Sensitive Material," Journal of Applied Mathematics and Physics (Zeitschrift für augewandte Mathematik und Physik), Vol. 21, 1970, pp. 1011-1032.

3 Lee, L. S. S., "Mode Responses of Dynamically Loaded Structures," JOURNAL OF APPLIED MECHANICS, Vol. 39, TRANS. ASME, Vol. 94, Series E, 1972, pp. 904-910.

4 Symonds, P. S., and Wierzbicki, T., "On an Extremum Principle for Mode Form Solutions in Plastic Structural Dynamics," JOURNAL OF APPLIED MECHANICS, Vol. 42, Series E, 1975, pp. 630-640.

5 Symonds, P. S., and Chon, C. T., "Approximation Techniques for Impulsive Loading of Structures of Time-Dependent Plastic Behavior with Finite Deflections," presented at the Conference on the Mechanical Properties of Materials at High Rates of Strain, Oxford University, April 2-4, 1974; Proceedings Mech. Props. of Mats. at High Strain Rates, Oxford Conference, Inst. Phys. Conf. Series No. 21, Dec. 1974.

6 Chon, C. T., and Symonds, P. S., "Large Dynamic Deflection of Plates by Mode Method," Journal of Engineering Mechanics Division, Proceedings, ASCE, Vol. 103, EM1, Feb. 1977, pp. 3-14.

7 Chon, C. T., and Martin, J. B., "A Rationalization of Mode Approximations for Dynamically Loaded Rigid-Plastic Structures Based on a Simple Model," Journal Structural Mechanics, Vol. 4(1), 1976, pp. 1-31.

8 Symonds, P. S., "Approximation Techniques for Impulsively Loaded Structures of Rate-Sensitive Plastic Behavior," SIAM Journal of Applied Mathematics, Vol. 25, No. 3, 1973.

9 Hopkins, H. G. and Prager, W., "The Load Carrying Capacity of Circular Plates," Journal Mechanics and Physics of Solids, Vol. 2, 1953, pp. 1-13.

10 Hopkins, H. G. and Prager, W., "On the Dynamics of Plastic Circular Plates," Journal of Applied Mathematics and Physics (ZAMP), Vol.V, 1954, pp. 317-330.

11 Wang, A. J. and Hopkins, H. G., "On the Plastic Deformation of Built-In Circular Plates under Impulsive Load," Journal of the Mechanics and Physics of Solids, 1954, Vol. 3, pp. 22-37.

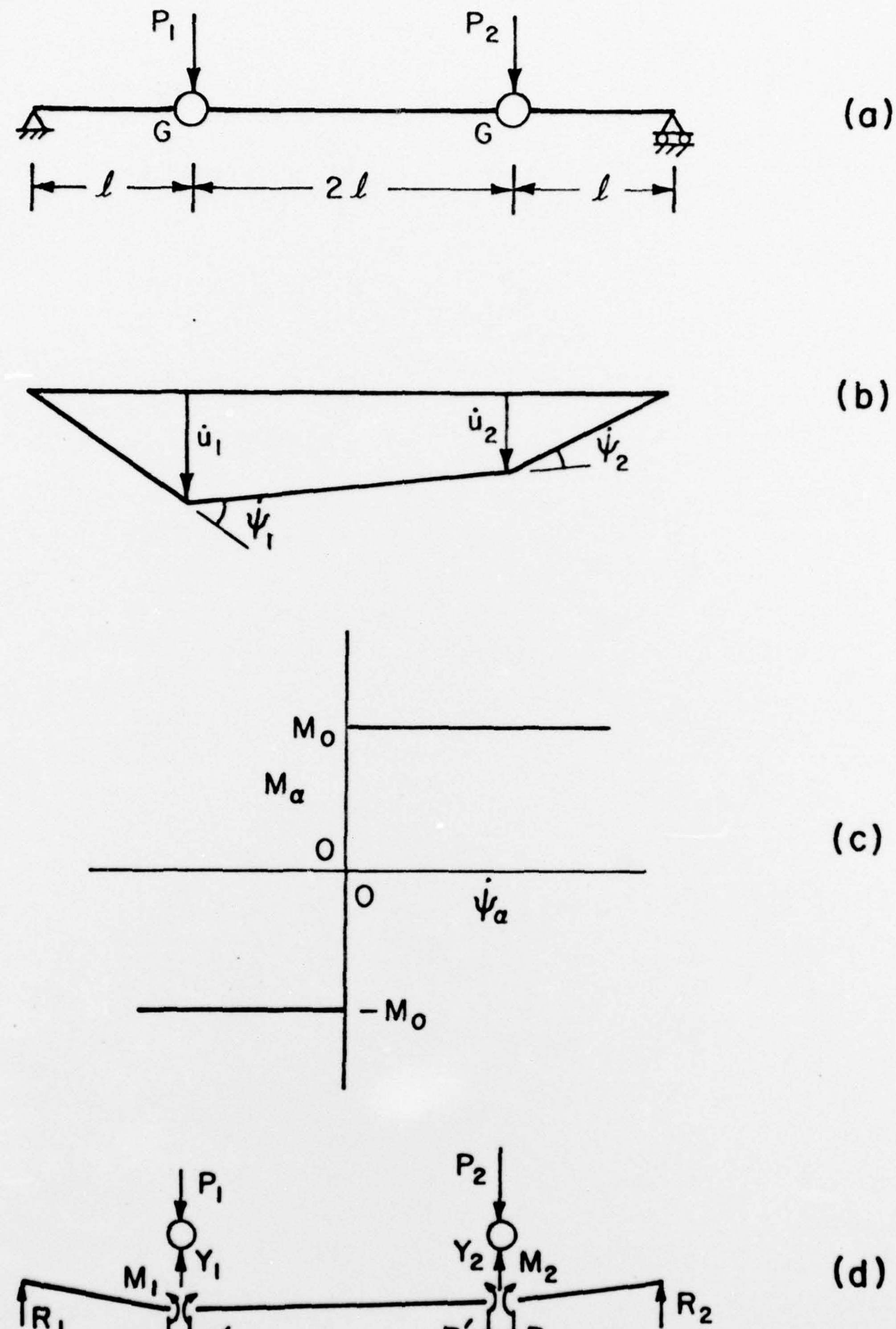


TWO-MASS MODEL

FIGURE 1

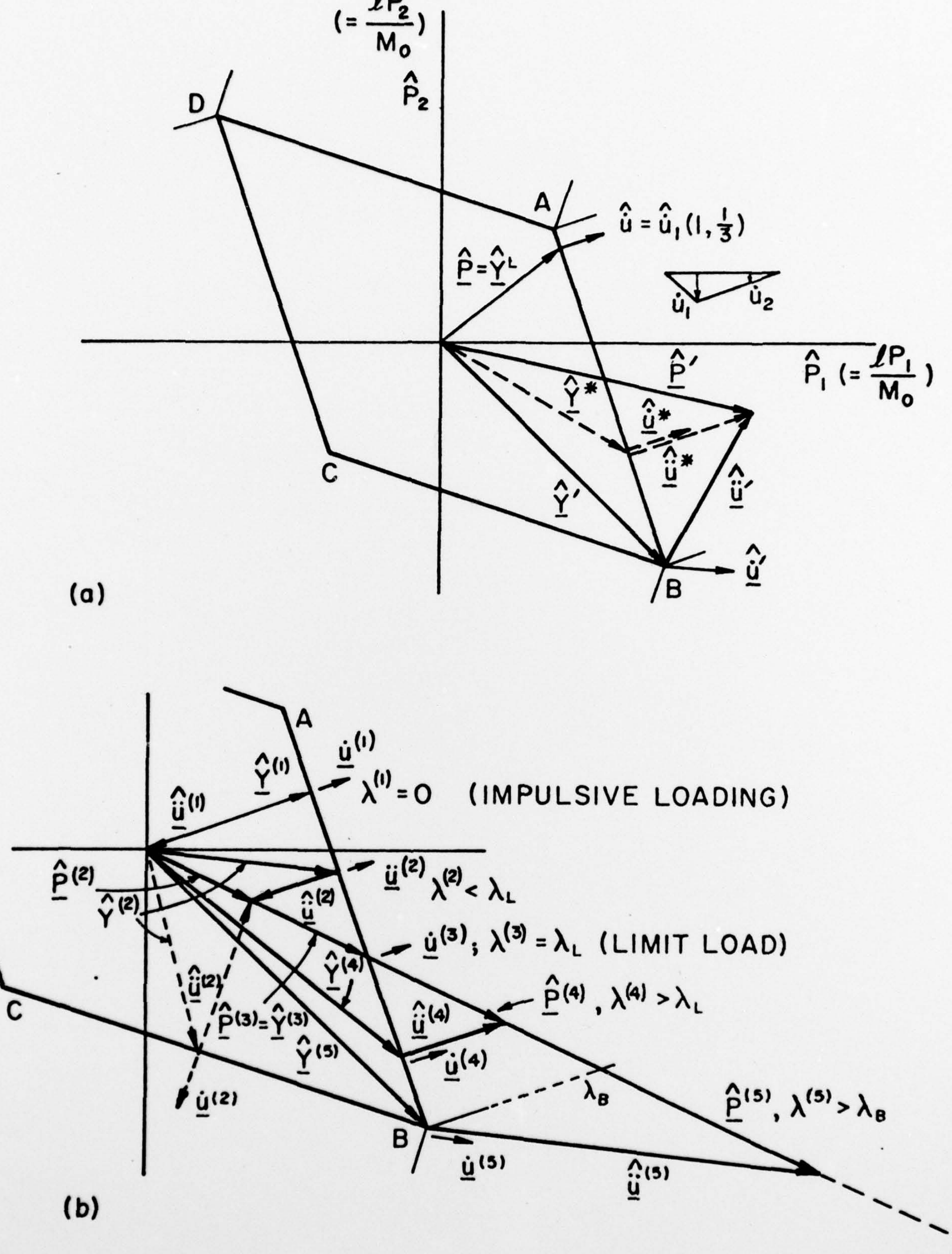


MODE FORM SOLUTIONS OF TWO MASS MODEL

FIGURE 2

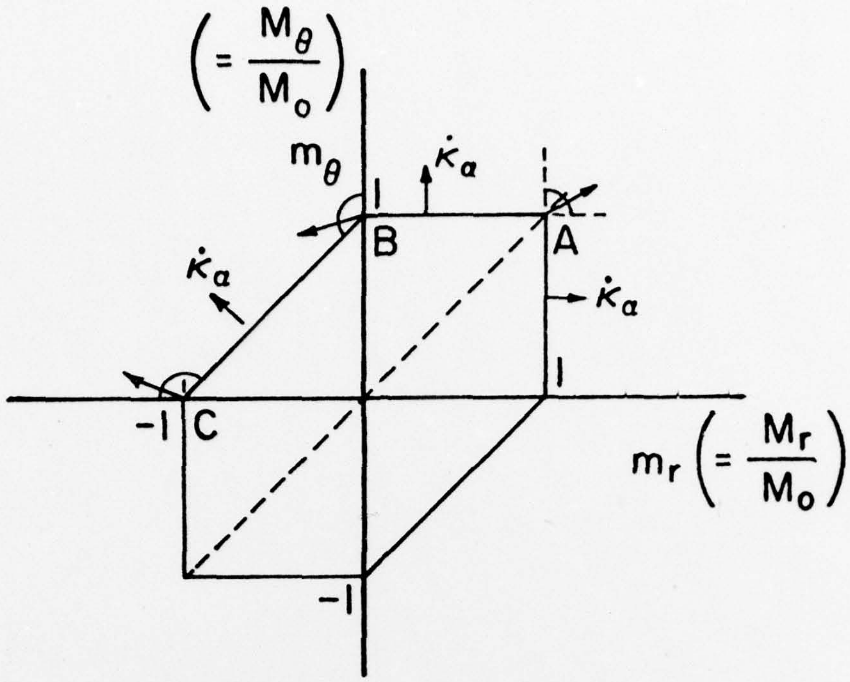


FIGURE 3

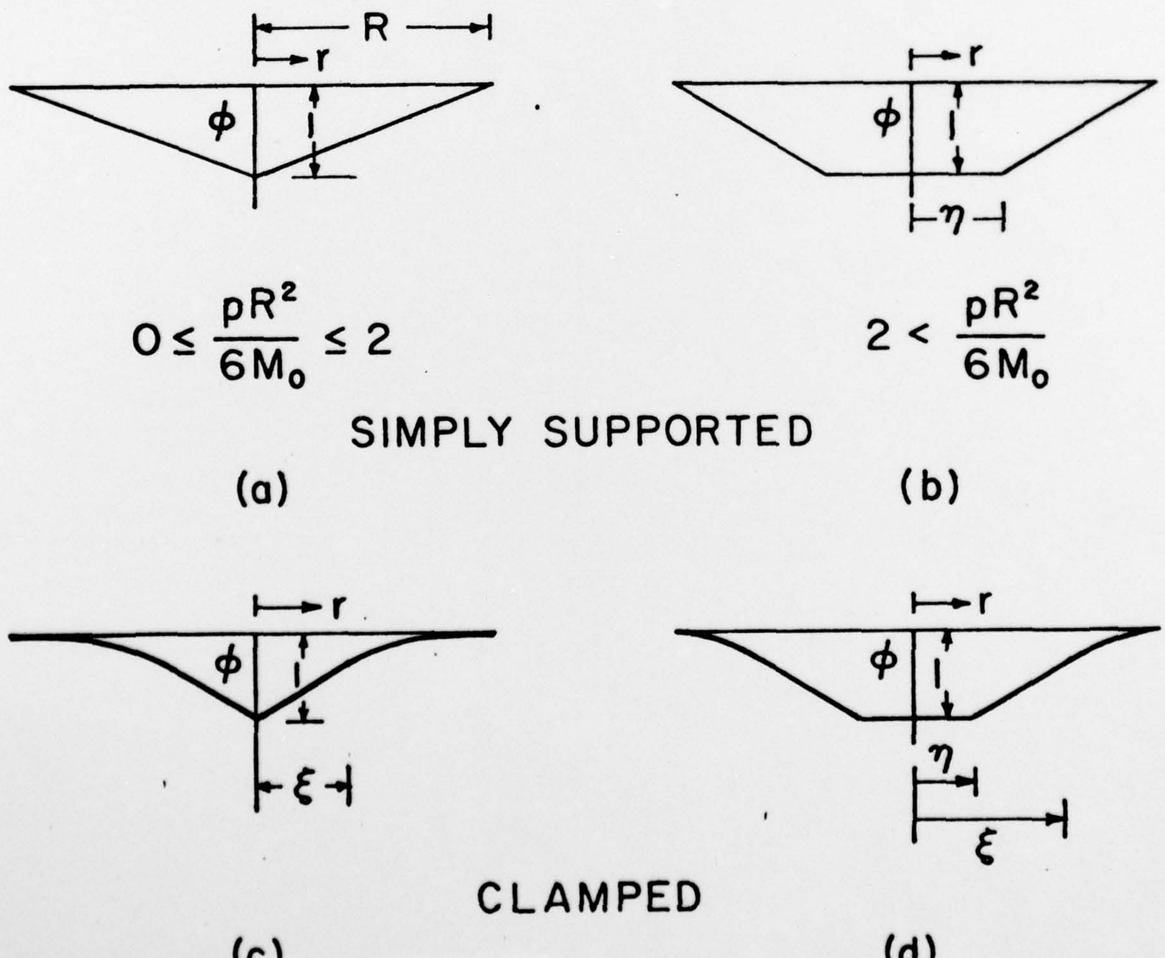


SHAPE FUNCTIONS $\phi(r)$ FOR PLATES OF TRESCA MATERIAL

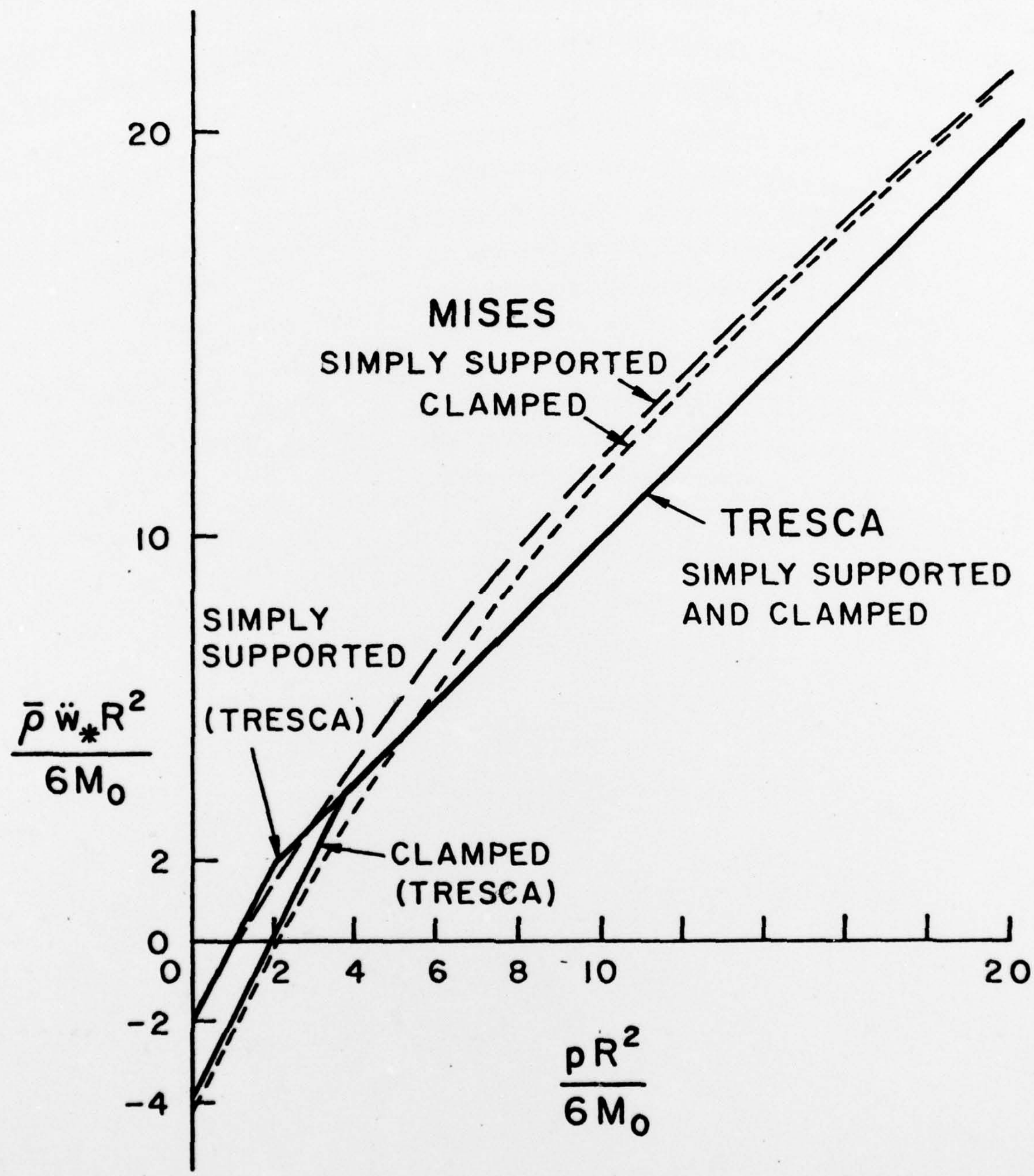

20
10
2
0
-2
-4
0
2
4
6
8
10
20
MISES
SIMPLY SUPPORTED
CLAMPED
TRESCA
SIMPLY SUPPORTED
AND CLAMPED
SIMPLY
SUPPORTED
(TRESCA)
CLAMPED
(TRESCA)
$\frac{\bar{\rho}\ddot{w}_* R^2}{6M_0}$
$\frac{pR^2}{6M_0}$


FIGURE 5

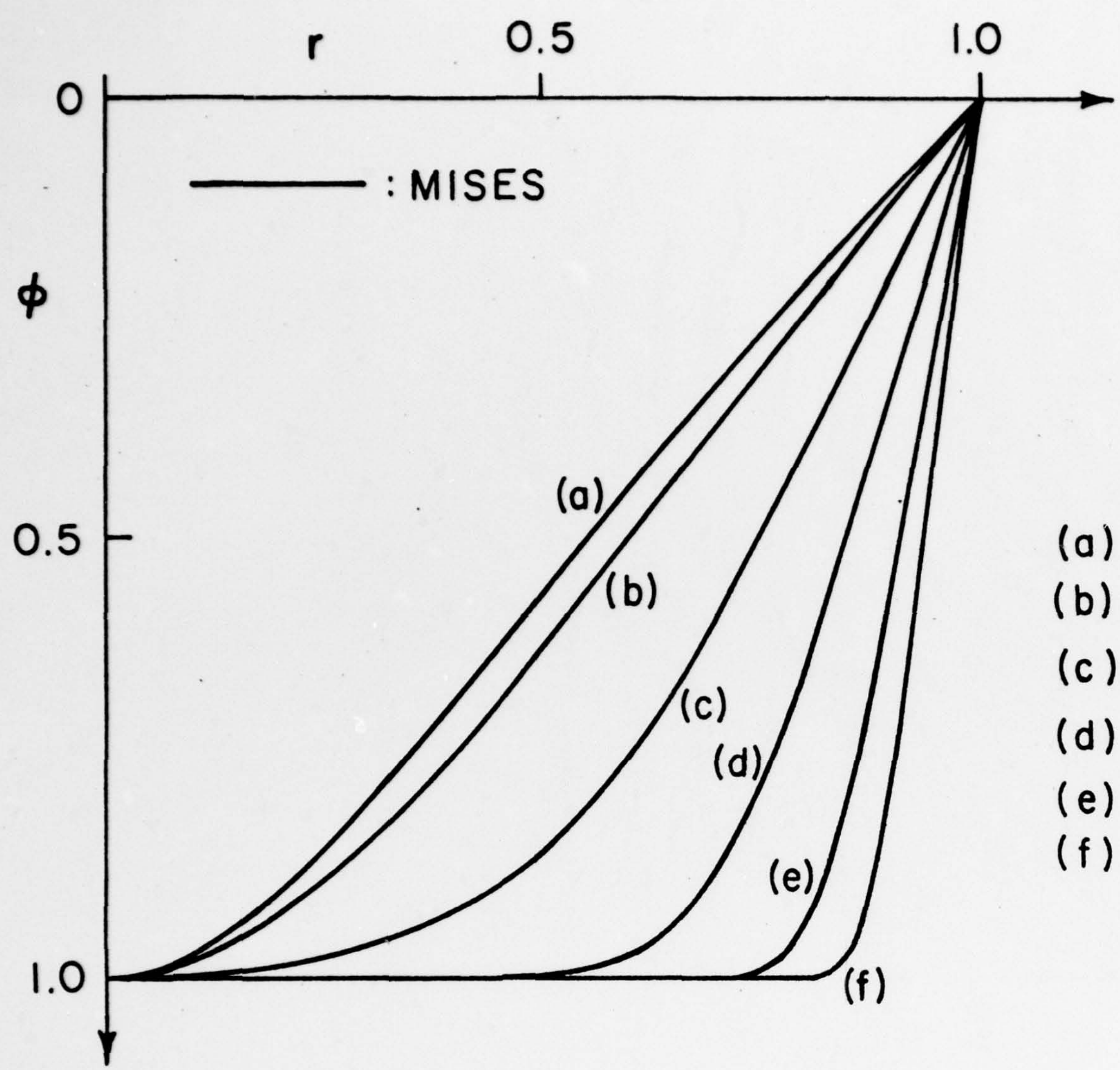


| | $\frac{PR^2}{6M_0}$ | $\frac{\bar{\rho} R^2 \ddot{w}_*}{6M_0}$ |
|---|---|---|
| (a) | 0 | -1.97 |
| (b) | 1.09 | 0.0 |
| (c) | 10 | 12.0 |
| (d) | 20 | 21.5 |
| (e) | 50 | 51.8 |
| (f) | 100 | 102 |

MODE SHAPES AND ACCELERATIONS
SIMPLY SUPPORTED CIRCULAR PLATE

FIGURE 6

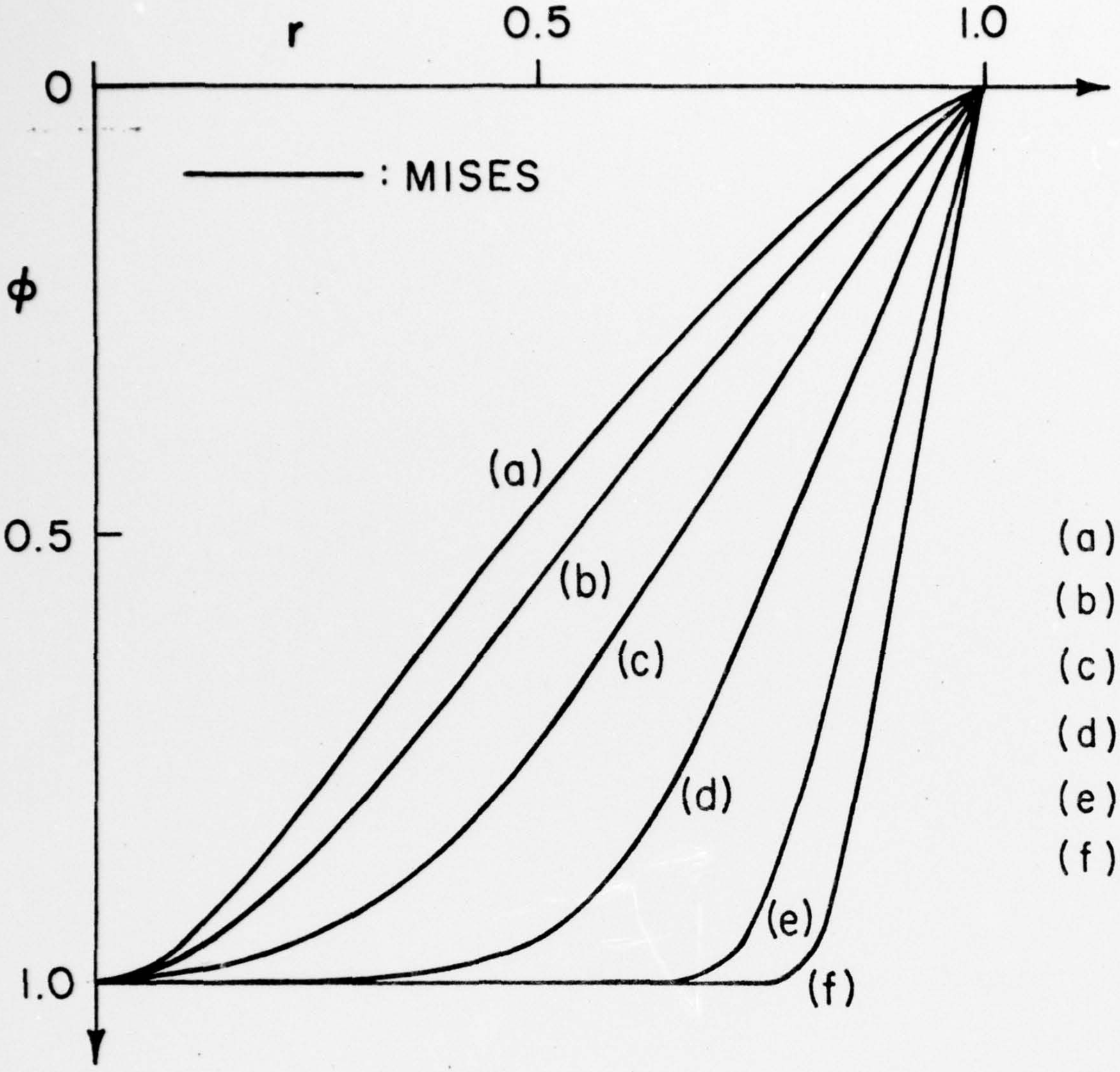


| | $\frac{PR^2}{6M_0}$ | $\frac{\bar{\rho}R^2\ddot{w}_*}{6M_0}$ |
|---|---|---|
| (a) | 0 | -4.21 |
| (b) | 2.10 | 0.0 |
| (c) | 10 | 11.7 |
| (d) | 20 | 21.8 |
| (e) | 50 | 51.5 |
| (f) | 100 | 102 |

MODE SHAPES AND ACCELERATIONS
CLAMPED CIRCULAR PLATE

FIGURE 7

SECURITY CLASSIFICATION OF THIS PAGE (*When Data Entered*)

| REPORT DOCUMENTATION PAGE | | READ INSTRUCTIONS BEFORE COMPLETING FORM |
|---|---|---|
| 1. REPORT NUMBER<br>(14) N00014-0860/2 | 2. GOVT ACCESSION NO. | 3. RECIPIENT'S CATALOG NUMBER |
| 4. TITLE (*and Subtitle*)<br>(6) ON DYNAMIC PLASTIC MODE FORM SOLUTIONS. | | 5. TYPE OF REPORT & PERIOD COVERED<br>(9) Technical rept. |
| | | 6. PERFORMING ORG. REPORT NUMBER |
| 7. AUTHOR(*s*)<br>(10) P. S. Symonds<br>C. T. Chon (now at Research Laboratory, General Motors Corporation) | | 8. CONTRACT OR GRANT NUMBER(*s*)<br>NSF-ENG74 21258<br>ONR N00014-75-C-0860 (15) |
| 9. PERFORMING ORGANIZATION NAME AND ADDRESS<br>Brown University, Division of Engineering<br>Providence, Rhode Island 02912 | | 10. PROGRAM ELEMENT, PROJECT, TASK AREA & WORK UNIT NUMBERS |
| 11. CONTROLLING OFFICE NAME AND ADDRESS<br>National Science Foundation, Washington, D. C. 20550<br>ONR, Arlington, Virginia 22217 | | 12. REPORT DATE<br>(11) June 1977<br>13. NUMBER OF PAGES<br>(12) 27 |
| 14. MONITORING AGENCY NAME & ADDRESS(*if different from Controlling Office*) | | 15. SECURITY CLASS. (*of this report*)<br>Unclassified<br>15a. DECLASSIFICATION/DOWNGRADING SCHEDULE |

16. DISTRIBUTION STATEMENT (*of this Report*)

DISTRIBUTION STATEMENT A
Approved for public release;
Distribution Unlimited

17. DISTRIBUTION STATEMENT (*of the abstract entered in Block 20, if different from Report*)

18. SUPPLEMENTARY NOTES

19. KEY WORDS (*Continue on reverse side if necessary and identify by block number*)

Mode, perfectly plastic, dynamic, engineering structure

20. ABSTRACT (*Continue on reverse side if necessary and identify by block number*) The paper discusses the significance and calculation of dynamic plastic mode form solutions for small deflections of structures of rigid-perfectly plastic materials subjected to load systems of fixed distribution and magnitude. These solutions have separated form, with velocity the product of a scalar function of time by a vector-valued function of space variables. The relation is shown on the one hand to mode form solutions for a structure of viscoplastic material, and on the other hand to limit load solutions for those of perfectly plastic behavior. Numerical examples are given for circular plates of material obeying Tresca and Mises' laws.

DD FORM 1 JAN 73 1473 EDITION OF 1 NOV 65 IS OBSOLETE
S/N 0102-014-6601

065 310